Local magnetic characterization of (Ga,Mn)As continuous thin film using scanning probe force microscopy

Inhee Lee, Yuri Obukhov, Jongjoo Kim, Xia Li, Nitin Samarth, Denis V. Pelekhov, and P. Chris Hammel

Phys. Rev. B **85**, 184402 — Published 2 May 2012

DOI: 10.1103/PhysRevB.85.184402

Local Magnetic Characterization of (Ga,Mn)As Continuous Thin Film Using Scanning Probe Force Microscopy

Inhee Lee,[1,*] Yuri Obukhov,[1] Jongjoo Kim,[1] Xia Li,[2] Nitin Samarth,[2] Denis V. Pelekhov,[1] and P. Chris Hammel[1,†]

[1]*Department of Physics, The Ohio State University, Columbus, OH, 43210, USA*
[2]*Department of Physics and Materials Research Institute, The Pennsylvania State University, University Park, Pennsylvania, 16802, USA*

(ΩDated: December 27, 2011)

We report spatially resolved measurements of the saturation magnetization, anisotropy field, and g-factor of a (Ga,Mn)As thin film using two different scanning probe techniques: Ferromagnetic Resonance Force Microscopy (FMRFM) and probe-induced Magnetic Force Microscopy (MFM). We find that the magnetic properties of the film are uniform within our 1 μm lateral resolution. We further demonstrate that these two powerful and complementary magnetic characterization approaches, the former dynamic and the latter static, obtain measurements of magnetic properties that are in excellent agreement with one another enabling enhanced quantitative reliability.

PACS numbers: 75.30.Ds, 75.75.Aa, 07.79.Pk, 76.50.Ag

I. INTRODUCTION

Ferromagnetic semiconductors, (Ga,Mn)As in particular[1–3], are attracting much attention for their potential importance in spintronic applications. The microscopic origins and fundamental physics of the ferromagnetism that occurs in these systems are under intense study. The ferromagnetism is strongly correlated with the concentration of hole carriers that mediate the interaction between Mn ions. This concentration primarily dependent on Mn concentration, is also sensitive to the concentration of point defects. Inhomogeneity can be introduced by a non-uniform Mn concentration[4] or variation of the carrier concentration. Local magnetic characterization of this material is important for better understanding of its physics and properties.

Here we report a spatially resolved study of the magnetic properties of (Ga,Mn)As thin film with a lateral resolution of $\sim 1\,\mu$m using both Ferromagnetic Resonance Force Microscopy (FMRFM)[5,6] and probe-induced Magnetic Force Microscopy (MFM)[7]. Ferromagnetic Resonance (FMR) measures the dynamical response of ferromagnetic magnetization allowing one to measure magnetic properties with spectroscopic precision; this makes it a powerful and widely used tool for measuring magnetic properties of ferromagnetic films and structures[8–12]. Magnetic Resonance Force Microscopy (MRFM)[13] provides detection of magnetic resonance with sensitivity sufficient to enable single electron spin detection[14] and high resolution nuclear magnetic resonance imaging of individual biomolecules[15]. This excellent sensitivity also allows FMR studies to be applied to individual ferromagnetic microstructures[5,16–18] and has recently enabled spatially resolved studies of extended samples[19,20]. Here we report quantitative, local magnetic characterization of a (Ga,Mn)As ferromagnetic thin film. We take advantage of an earlier theory[21] to calculate the magnetic resonance force signal arising from the uniform FMR mode excited in the region affected by the inhomogeneous magnetic field of the micromagnetic probe tip. This force signal contains quantitative information about the magnetic properties of the film beneath the magnetic probe, while the resonance spectrum reveals properties of the spatially extended uniform FMR mode.

A novel MFM method, probe-induced Magnetic Force Microscopy,[7], enables quantitative characterization of ferromagnetic films with lateral resolution defined by the probe-sample separation and probe size. This technique employs a strong external field to saturate the film and exploits the known perturbation of the sample magnetization by the localized magnetic field (0.5–3 kG) of the high coercivity probe magnet. The non-uniform magnetization of the sample induced by the probe magnetic field generates an MFM signal which yields quantitative characterization of the magnetic properties of the ferromagnetic film.

Here we present measurements of the saturation magnetization, anisotropy field, and g-factor of the film obtained using these two complementary approaches. We show that comparison of the FMRFM and probe-induced MFM results yields excellent agreement indicating that this two-pronged approach offers reliable, quantitative measurement of ferromagnetic film characteristics with lateral resolution defined by the magnetic probe size.

II. EXPERIMENTAL DETAILS

The (Ga,Mn)As thin film was grown on a GaAs substrate to a thickness of 50 nm with a 3–5% Mn doping level producing a Curie temperature $T_c = 100$ K and saturation magnetization $M_s = 38\,\mathrm{emu/cm^3}$ measured by SQUID magnetometry at 10 K. The FMRFM and probe-induced MFM were performed at $T \sim 10$ K in vacuum. The (Ga,Mn)As film was positioned on a stripline microwave resonator operating at 7.475 GHz. An external magnetic field $\mathbf{H_0}$ large enough to saturate the film magnetization was applied perpendicular to the film plane (in

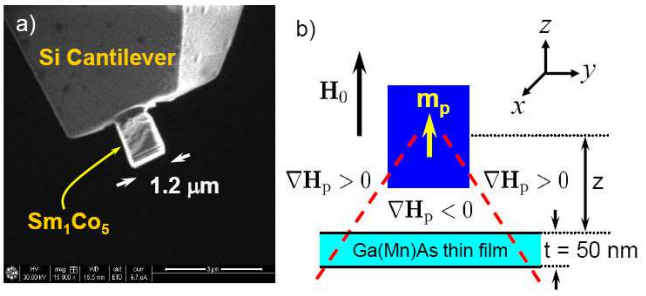

FIG. 1: (a) Micrograph of the $SmCo_5$ probe magnet shaped using a focused ion beam. (b) Schematic diagram of our experiment: $\mathbf{H_0}$ is the external field applied perpendicular to the (Ga,Mn)As film plane; $\nabla\mathbf{H_p}$ is the probe field gradient; $\mathbf{m_p}$ is the magnetic moment of the probe magnetized parallel to $\mathbf{H_0}$; and t is the film thickness. The dashed lines define regions where the probe field gradient changes sign.

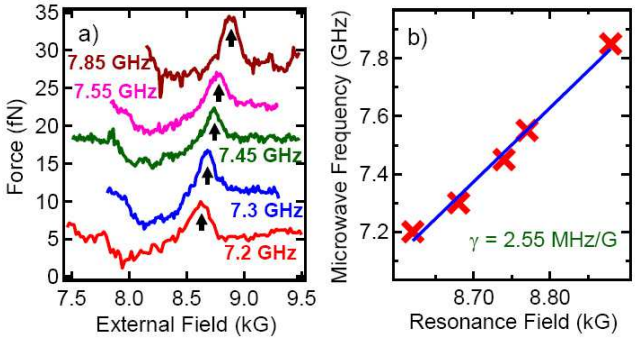

FIG. 2: (a) FMRFM spectra at different microwave frequencies measured at a probe-sample separation $z = 1430$ nm. The arrows indicate the uniform FMR mode resonance field. The FMRFM spectra are vertically offset for clarity. (b) Dependence of microwave frequency on resonance field taken from (a) (red crosses). The slope of the linear fit, shown by the line, gives the gyromagnetic ratio for the (Ga,Mn)As film: γ = 2.55 MHz/G.

the $\hat{z}$-direction). The experimental geometry is shown in Fig. 1(b). The $SmCo_5$ micromagnetic probe shown in Fig. 1(a) was glued on a commercially available Si cantilever and shaped to a $\sim 1.2 \times 1.2 \times 1.5\,\mu\text{m}^3$ block using a focused ion beam. The resonance frequency and spring constant of the cantilever are 13.2 kHz and ≈ 0.14 N/m respectively. The probe moment $m_p \approx 1.2 \times 10^{-9}$ emu is parallel to $\mathbf{H_0}$ and the probe's coercivity exceeds 2 T.

In the FMRFM experiment, we apply a microwave field $\mathbf{h_1}$ perpendicular to $\mathbf{H_0}$. The resulting FMR excitation suppresses the z-component of the film magnetization thus reducing the probe-sample force. We modulate the microwave power at the cantilever frequency and measure the resulting force response of the cantilever oscillating at its eigenfrequency. The details of the method and detection scheme are described in detail elsewhere[18,19,22]. The modulation of the microwave amplitude is typically 60%. In the probe-induced MFM experiments the microwave power is off and we monitor the MFM force gradient at different probe sample separations using the same frequency detection scheme[7,22].

III. RESULTS AND DISCUSSION

A. Ferromagnetic Resonance Force Microscopy (FMRFM)

As expected, the resonance field of the FMRFM signal of the uniform FMR mode[17–19,23] shown in Fig. 2 is independent of probe-sample separation. In the absence of a spatially modulated FMR response, the force between the probe and unperturbed uniform FMR mode will be zero (just as the MFM force from a uniformly magnetized thin film vanishes). However, because the localized and intense magnetic field of the probe alters the local resonance frequency, the uniform FMR mode is partially or completely suppressed just beneath the probe. This results in a non-zero FMRFM force[21] whose magnitude is reflective of the magnetic properties of the film beneath the probe. The FMR resonance field, obtained from the peaks indicated by the arrows such as shown in Fig. 2(a), is insensitive to the probe-sample separation. This might be unexpected since reducing this separation increases the probe field experienced by the film immediately below. However, because the observed signal arises from laterally distant regions of the film where the probe field is negligible the resonance is not shifted.

The gyromagnetic ratio γ was determined by measuring the dependence of FMRFM resonance field on microwave frequency as shown in Fig. 2(a): $\omega/\gamma = H_0 - 4\pi M_s + H_{a\perp}$ where $\omega/2\pi$ is the microwave frequency, H_0 is the applied external magnetic field, M_s is the saturation magnetization of the sample, $-4\pi M_s$ is the demagnetizing field for the film and $H_{a\perp}$ is the perpendicular crystalline anisotropy field. From the slope of the linear fit of resonance field to frequency in Fig. 2(b), we obtain $\gamma = 2.55 \pm 0.14$ MHz/G, corresponding to $g = 1.82 \pm 0.1$, close to previously reported values[24,25]. We find that $4\pi M_s - H_{a\perp} \approx 5.82$ kG. SQUID-magnetometry gives $M_s = 38\,\text{emu/cm}^3$, so we can infer $H_{a\perp} \approx -5.34$ kG. This is larger than reported values of ~ 3 kG typically reported for similar (Ga,Mn)As samples[25,26]. However, the authors of Ref. 27 show that increasing hole concentration reduces the g-factor and this, in turn, is associated with a stronger perpendicular anisotropy field. Our larger perpendicular anisotropy field agrees well with this result if we take into account our relatively lower g-factor[25,26].

Next we consider the magnitude of the uniform FMR mode force peak. If the amplitude of the dynamic magnetization m_0 of the uniform mode is constant across the thickness of the film, m_0 is determined by the microwave field h_1 and FMR linewidth ΔH arising from

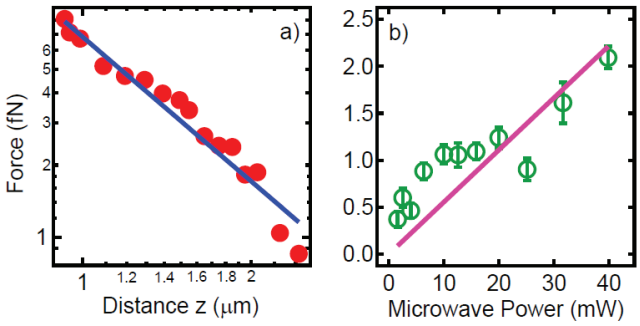

FIG. 3: (a) FMRFM force magnitude for the uniform FMR mode as a function of probe-sample separation z. The line shows the fit of the experimental data to Eq. 3. (b) Microwave power dependence of FMRFM force magnitude measured at $z = 1470$ nm. The line shows the best linear fit to Eq. 3.

the Gilbert damping and inhomogeneous broadening in the ferromagnetic sample:

$$M_s h_1 = m_0 \Delta H \tag{1}$$

The intense, localized probe field suppresses the uniform FMR mode beneath the probe, and the degree of the suppression depends on the probe-sample separation as shown in Ref. 21. This suppression is partial for $z \gtrsim \sqrt{2m_p/\pi M_s t \beta_0} \approx 12.8\,\mu$m for our sample ($\beta_0 \approx 2.405$ is the first zero of the Bessel function $J_0(\beta_0) = 0$), and is full for $z \lesssim \sqrt{2m_p/\pi M_s t \beta_0}$. The experimental data reported here were measured in the latter z-range, so the FMR mode is fully suppressed under the probe; in this regime the FMRFM force is given by[21]

$$F(z, m_0) = -\frac{2\pi m_0^2 t}{3^{3/2} M_s} \frac{m_p}{z^2} \tag{2}$$

The radius of the suppressed region in this case is $\delta r = \sqrt{2} z$. Using Eqs. 1 and 2, the FMRFM force can then be rewritten:

$$F(z, P) = -\frac{2\pi m_p M_s t}{3^{3/2} (\Delta H)^2} \frac{\alpha P}{z^2} \tag{3}$$

where $\Delta H \approx 150$ G is the FMR linewidth, P is microwave power, and α is a parameter relating P and microwave field generation in the stripline resonator: $\alpha P = h_1^2$. Fig. 3 compares experimental data to Eq. 3: Fig. 3(a) shows that the FMRFM force dependence on separation z is well described by the predicted power law $F \propto 1/z^2$, and Fig. 3(b) demonstrates the expected dependence of the force signal on microwave power. Using our experimental data we can determine M_s from Eq. 3 if we know the microwave field h_1. We obtain $M_s \approx 39.8 \pm 0.9$ emu/cm^3 for a microwave field $h_1 \approx 0.74$ G. Conversely, if we know the value M_s, we can obtain the value of microwave field h_1. This procedure allows us to map M_s with lateral resolution defined by probe sample separation $\delta r \approx \sqrt{2}\, z$ or the probe radius, whichever is larger. In contrast, the spectral response of the FMRFM signals arises from outside the region of radius $\delta r = \sqrt{2}\, z$ centered immediately beneath the probe tip. Our spatial maps of M_s and $4\pi M_s - H_{a\perp}$ from FMRFM force measurements and from spectroscopy in a scanning area $10 \times 10\,\mu$m^2 show the saturation magnetization and the magneto-crystalline anisotropy field to be uniform.

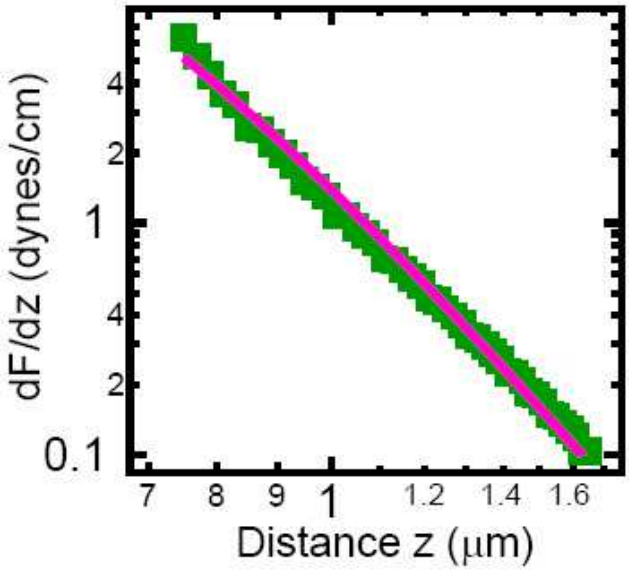

FIG. 4: The dependence of the probe-induced MFM force gradient on probe sample separation z, measured at $H_0 = 8.74$ kG. The line shows the fit to the experimental data using Eq. 5. The force gradient exhibits the expected power law dependence: $dF/dz \propto 1/z^6$.

B. Probe-induced magnetic force microscopy

Conventional MFM typically employs a sharp tip that produces a weak magnetic field in order to minimize the perturbation of the sample magnetization while achieving excellent lateral resolution. This makes it an excellent tool for imaging spatially inhomogeneous magnetic features such as domain walls and sample discontinuities. However, because the force exerted on the probe by a uniformly magnetized film vanishes[28], this approach is difficult to use with nearly homogeneous extended films. We circumvent this problem by using a probe magnet that generates fields up to 2 kG at small probe-sample separations, sufficient to induce an inhomogeneous sample magnetization. This generates a non-zero force between the probe and the extended sample as discussed in Ref. 7 and allows quantitative measurement of the magnetic sample properties. This probe-induced MFM force

TABLE I: Comparison of measured parameter values

Method	M_s (emu/cm^3)	$4\pi M_s - H_{a\perp}$ (kG)	Spatial Resolution
FMRFM spectroscopy		5.82	
FMRFM force	39.8		$\sqrt{2}\,z$
Probe-induced MFM	39.3	5.7	z

(see Eq. 2 in Ref. 7) is given by:

$$F_z = M_s t \int_S \left(\frac{\partial}{\partial z} H_{p\perp} + \frac{H_{t\parallel}}{H_{t\perp}} \frac{\partial}{\partial z} H_{p\parallel} \right) dS \qquad (4)$$

where $H_{p\parallel}$ and $H_{p\perp}$ are the parallel and perpendicular components of the probe field relative to sample plane, $H_{t\parallel}$ and $H_{t\perp}$ are the parallel and perpendicular components of the total internal field, and S is the sample area. For a thin magnetic film saturated in a strong, out-of-plane magnetic field H_0 in the presence of a micromagnetic probe $H_{t\perp} \approx H_0 - 4\pi M_s + H_{a\perp} + H_{p\perp}$ and $H^t_{||} \approx H_{p\parallel}$. Here we disregard the parallel component of demagnetizing field for a thin film, and the exchange field for probe-sample distance greater than 100 nm. The term $F_z^{(I)} = M_s t \int_S \frac{\partial}{\partial z} H^p_\perp dS$ in Eq. 4 describes the force between the probe and the sample uniformly saturated in the external field $\mathbf{H}_0$. For an infinite thin film sample having uniform saturation magnetization M_s, this term will be zero. The second term $F_z^{(II)} = M_s t \int_S (H^p_{||}/H^t_\perp) \frac{\partial}{\partial z} H^p_{||} dS$ in Eq. 4 describes the interaction of the probe with the in-plane component of the probe-induced sample magnetization. The resulting force gradient is given by differentiating Eq. 4 with respect to z:

$$\begin{aligned} \frac{dF_z}{dz} &= M_s t \frac{\partial}{\partial z} \int_S \left(\frac{H_{p\parallel}}{H_0 - 4\pi M_s + H_{a\perp} + H_{p\perp}} \frac{\partial H_{p\parallel}}{\partial z} \right) dS \\ &\approx \frac{15\pi}{2} \frac{M_s t}{H_0 - 4\pi M_s + H_{a\perp}} \frac{m_p^2}{z^6}. \end{aligned} \qquad (5)$$

The latter expression assumes the probe can be treated as a point dipole and that $H_{p\perp}$ can be neglected in the denominator. This expression can interpreted as the interaction of the probe magnet with the effective dipole moment $m_{\rm ind}$ induced in the film by the probe magnetic field in an area with characteristic radius $\delta r \sim z$. This magnetic moment is given by

$$m_{\rm ind} = \frac{5\pi}{16} \frac{M_s t}{H_0 - 4\pi M_s + H_{a\perp}} \frac{m_p}{z}.$$

Fig. 4 shows the dependence of the probe-induced MFM force gradient on probe-sample separation z in an external field $H_0 = 8.74$ kG. The fit of Eq. 5 to the experimental data is quite good: the data exhibits the expected power law $dF/dz \propto 1/z^6$ in spite of the presence of spurious probe-sample forces (e.g., electrostatic or Van der Waals). This fit gives $H_{a\perp} = -5.2$ kG, and $M_s = 39.3$ emu/cm^3, in excellent agreement with the result obtained using FMRFM.

C. Complementarity of FMRFM and probe-induced MFM methods

Table I summarizes the magnetic measurements obtained using the two scanned probe magnetic microscopy methods. Each has particular strengths and the combination of the two approaches provides a powerful approach to obtaining reliable quantitative measurements. FMRFM spectroscopy determines $4\pi M_s - H_{a\perp}$ with spectroscopic precision. FMRFM force measurements give M_s; however the need for knowledge of h_1 and accurate determination of FMR linewidth ΔH introduces uncertainty into the determination of M_s. Although the accuracy of probe-induced MFM can be degraded by non-magnetic forces between probe and sample, probe-induced MFM can provide a reliable determination of local M_s independent of $H_{a\perp}$. The strong dependence of the probe-induced MFM force gradient on distance ($\partial F/\partial z \propto 1/z^6$) means that accurate measurement of z is essential.

FMRFM and probe-induced MFM are complementary methods for measuring magnetic properties. We find that applying them together enables improved accuracy in spatially mapping the magnetic properties of films. Given the sensitivity of the magnetism of (Ga,Mn)As to quantities such as hole concentration and defects, this approach is particularly attractive for measuring the potentially spatially varying quantities to better understand results obtained in various experiments. We find excellent agreement between results obtained using these two independent techniques measured under identical conditions, thus confirming the power of combining these measurement approaches to spatial mapping of magnetic properties with improved reliability.

IV. CONCLUSIONS

Our spatially resolved study of the magnetic properties of a (Ga,Mn)As thin film using the complementary techniques of scanned probe FMR (FMRFM) and probe-induced MFM, performed with a lateral resolution of $\delta r \sim 1\,\mu$m, shows its saturation magnetization, anisotropy field and g-factor to be uniform on this length scale. We find that $M_s = 39.3\,$emu/cm^3, $H_{a\perp} = -5.34$ kG, and g-factor $g = 1.82$. We further find that apply-

ing FMRFM and probe-induced MFM together enables a detailed, quantitative and reliable determination of ferromagnetic film quantities with lateral resolution defined by the magnetic probe size. This work was supported by the US Department of Energy through grant DE-FG01-03ER46054, and by the NSF through both the MRSEC program, grant DMR-0820414, and grant DMR-0801406.

* Electronic address: ilee@bnl.gov
† Electronic address: hammel@physics.osu.edu

[1] H. Ohno, Science **281**, 951 (1998).
[2] T. Jungwirth, J. Sinova, J. Maek, J. Kuera, and A. H. MacDonald, Reviews of Modern Physics **78**, 809 (2006).
[3] A. H. MacDonald, P. Schiffer, and N. Samarth, Nature Mater. **4**, 195 (2005).
[4] J. Shi, J. M. Kikkawa, R. Proksch, T. Schaffer, D. D. Awschalom, G. Medeiros-Ribeiro, and P. M. Petroff, Nature **377**, 707 (1995).
[5] Z. Zhang, P. C. Hammel, and P. E. Wigen, Applied Physics Letters **68**, 2005 (1996).
[6] P. C. Hammel and D. V. Pelekhov, in *Handbook of Magnetism and Advanced Magnetic Materials*, edited by H. Kronmüller and S. Parkin (John Wiley & Sons, Ltd., New York, NY, 2007), Vol. 5, Chap. 4.
[7] I. Lee, J. Kim, Y. Obukhov, P. Banerjee, D. V. Pelekhov, A. Hauser, F. Yang, and P. C. Hammel, Appl. Phys. Lett. **99**, 162514 (2011).
[8] A. Hubert and R. Schafer, *Magnetic Domains. The analysis of magnetic Microstructures* (Springer, Berlin, 1998), pp. 78–85.
[9] X. Liu and J. K. Furdyna, J. Phys.: Condens. Matter **18**, R245 (2006).
[10] K. Y. Guslienko, R. W. Chantrell, and A. N. Slavin, Phys. Rev. B **68**, 024422 (2003).
[11] G. N. Kakazei, P. E. Wigen, K. Y. Guslienko, V. Novosad, A. N. Slavin, V. O. Golub, N. A. Lesnik, and Y. Otani, Appl. Phys. Lett. **85**, 443 (2004).
[12] G. N. Kakazei, Y. G. Pogorelov, M. D. Costa, T. Mewes, P. E. Wigen, P. C. Hammel, V. O. Golub, T. Okuno, and V. Novosad, Phys. Rev. B **74**, 060406 (2006).
[13] D. Rugar, C. S. Yannoni, and J. A. Sidles, Nature **360**, 563 (1992).
[14] D. Rugar, R. Budakian, H. J. Mamin, and B. W. Chui, Nature **430**, 329 (2004).
[15] C. L. Degen, M. Poggio, H. J. Mamin, C. T. Rettner, and D. Rugar, Proc. Natl. Acad. Sci. USA **106**, 1313 (2009).
[16] G. de Loubens, V. V. Naletov, O. Klein, J. B. Youssef, F. Boust, and N. Vukadinovic, Physical Review Letters **98**, 127601 (2007).
[17] T. Mewes, J. Kim, D. V. Pelekhov, G. N. Kakazei, P. E. Wigen, S. Batra, and P. C. Hammel, Physical Review B **74**, 144424 (2006).
[18] Y. Obukhov, D. V. Pelekhov, J. Kim, P. Banerjee, I. Martin, E. Nazaretski, R. Movshovich, S. An, T. J. Gramila, S. Batra, and P. C. Hammel, Physical Review Letters **100**, 197601 (2008).
[19] I. Lee, Y. Obukhov, G. Xiang, A. Hauser, F. Yang, P. Banerjee, D. V. Pelekhov, and P. C. Hammel, Nature **466**, 845 (2010).
[20] E. Nazaretski, I. Martin, R. Movshovich, D. V. Pelekhov, P. C. Hammel, M. Zalalutdinov, J. W. Baldwin, B. Houston, and T. Mewes, Applied Physics Letters **90**, 234105 (2007).
[21] Y. Obukhov, D. V. Pelekhov, E. Nazaretski, R. Movshovich, and P. C. Hammel, Applied Physics Letters **94**, 172508 (2009).
[22] Y. Obukhov, K. C. Fong, D. Daughton, and P. C. Hammel, Journal of Applied Physics **101**, 034315 (2007).
[23] E. Nazaretski, I. Martin, R. Movshovich, D. V. Pelekhov, P. C. Hammel, M. Zalalutdinov, J. W. Baldwin, B. Houston, and T. Mewes, Appl. Phys. Lett. **90**, 234105 (2007).
[24] X. Liu, W. L. Lim, L. V. Titova, M. Dobrowolska, J. K. Furdyna, M. Kutrowski, and T. Wojtowicz, Journal of Applied Physics **98**, 063904 (2005).
[25] A. Wirthmann, X. Hui, N. Mecking, Y. S. Gui, T. Chakraborty, C. M. Hu, M. Reinwald, C. Schüller, and W. Wegscheider, Applied Physics Letters **92**, 232106 (2008).
[26] X. Liu, Y. Sasaki, and J. K. Furdyna, Physical Review B **67**, 205204 (2003).
[27] X. Liu, W. L. Lim, M. Dobrowolska, J. K. Furdyna, and T. Wojtowicz, Physical Review B **71**, 035307 (2005).
[28] J. J. Saenz, N. Garcia, P. Grutter, E. Meyer, H. Heinzelmann, R. Wiesendanger, L. Rosenthaler, H. R. Hidber, and H.-J. Guntherodt, Journal of Applied Physics **62**, 4293 (1987).